Monte Carlo simulations of complex formation between a mixed fluid vesicle and a charged colloid

Miha Fošnarič,[1,a)] Aleš Iglič,[1] Daniel M. Kroll,[2] and Sylvio May[2]
[1]*Faculty of Electrical Engineering, University of Ljubljana, Tržaška 25, 1000 Ljubljana, Slovenia*
[2]*Department of Physics, North Dakota State University, Fargo, North Dakota 58105-5566, USA*

(Received 6 May 2009; accepted 2 July 2009; published online 10 September 2009)

Monte Carlo simulations are employed to investigate the ability of a charged fluidlike vesicle to adhere to and encapsulate an oppositely charged spherical colloidal particle. The vesicle contains mobile charges that interact with the colloid and among themselves through a screened electrostatic potential. Both migration of charges on the vesicle surface and elastic deformations of the vesicle contribute to the optimization of the vesicle-colloid interaction. Our Monte Carlo simulations reveal a discontinuous wrapping transition of the colloid as a function of the number of charges on the vesicle. Upon reducing the bending stiffness of the vesicle, the transition terminates in a critical point. At large electrostatic screening length we find a reentrant wrapping-unwrapping behavior upon increasing the total number of charges on the vesicle. We present a simple phenomenological model that qualitatively captures some features of the wrapping transition. © *2009 American Institute of Physics*. [doi:10.1063/1.3191782]

I. INTRODUCTION

Cellular membranes serve as a permeability barrier to large water-soluble macroions. However, intra- and extracellular transport of such macroions is still possible by a dynamic membrane remodeling that generally involves membrane bending deformations. In some cases, such as receptor-mediated endocytosis, the membrane deformation is tightly regulated by a molecular machinery and requires a metabolic energy source. For example, clathrin-mediated endocytosis relies on the auxiliary protein clathrin to control the size of the coated transport vesicles. In other cases, the membrane deformation progresses passively, i.e., without employing an additional energy source, driven solely by the interaction between the membrane and the macroion. Examples include the viral budding of newly formed virions out of their host cells[1] and the transfer of drug delivery vehicles into cells. Liposomes often serve as such vehicles for encapsulated material.[2] For example, it has been reported that small cationic liposomes attach to negatively charged membranes and induce strong local membrane bending, resulting in liposome encapsulation.[3] Of interest is also the nonviral entry of genetic material into cells based on self-assembled condensed complexes of DNA with a carrier material. To form sufficiently compact aggregates, DNA can be complexed with cationic lipids or cationic polymers; both cases result in positively charged condensates that electrostatically interact with the plasma membrane[4] and are typically internalized in a nonspecific manner (i.e., by macropinocytosis). Note that all these transport mechanisms involve, at some stage, a curved membrane that engulfs a charged colloidal particle, liposome, or aggregate.

Colloidal particles enveloped by lipid membranes also have promising biotechnological applications, including their use as analytical essays and biofunctionalized surfaces.[5] However, stability of the lipid shell often limits the control of surface properties. Recent research efforts have therefore been directed toward introducing chemical modifications that improve the stability of lipid-coated colloidal particles. In addition, physical properties such as the surface topography and particle sizes contribute to the properties of membrane-colloid complexes. Understanding the interplay of the various energy contributions, including elastic and electrostatic energies of the colloid-membrane complexes, is a prerequisite for improving complex stability.

The wrapping of colloidal particles by fluid membranes has been considered in previous theoretical studies. Harries *et al.*[6] used the nonlinear Poisson–Boltzmann model to investigate the enveloping of charged proteins by initially planar lipid membranes, thereby accounting for the protein-induced demixing of the charged lipids in a binary membrane. A comparison of the free energies corresponding to the fully wrapped and unwrapped states suggested that wrapping occurs only above a critical protein charge. That critical protein charge is compatible with the number of charges typically contained in membrane-penetrating peptide shuttles. In another study, Fleck and Netz[7] modeled the electrostatic colloid-membrane binding by minimizing the free energy of a homogeneously charged membrane with respect to the membrane shape using the screened Debye–Hückel potential. The authors found a reentrant unwrapping behavior, where small and large salt concentrations lead to a small degree of wrapping. This occurs because for large salt concentration electrostatic screening reduces the membrane-colloid interaction, whereas for small salt concentrations unwrapping is due to the self-energy of the membrane. For intermediate salt concentrations, however, wrapping becomes almost complete. In a series of studies, Deserno and co-worker[8–10] analyzed the engulfment of colloids by mem-

[a)]Electronic mail: miha.fosnaric@fe.uni-lj.si.

branes in the presence of a short-ranged (adhesive) interaction potential. In this case, the deformation of an initially flat membrane is determined by an interplay of bending energy and interfacial tension, and the wrapping transition is generally predicted to proceed discontinuously, jumping from a partially to a completely wrapped binding state of the colloid. If the membrane contains a binary mixture of lipids with opposite spontaneous curvatures, wrapping will be facilitated by local lipid demixing.[11] Demixing is also important if a colloidal particle binds to mobile adhesion sites as is the case in the receptor-mediated uptake of viruses.[12] The cellular entry of viruses through the endocytotic pathway provides a major motivation to refine models of colloid-membrane complexes.[13,14] Simulations of colloid engulfment by membranes have been performed using dissipative particle dynamics[15] and a solvent-free coarse-grained membrane model.[16]

In this work we present the Monte Carlo simulations of electrostatically driven colloid adhesion and wrapping by a fluid binary vesicle. We represent the vesicle by a randomly triangulated surface, and we use the linear Debye–Hückel potential to describe electrostatic interactions. The vesicle and colloid contain opposite charges; those attached to the colloid are immobile, whereas the vesicle charges are able to diffuse within the vesicle's surface. When interacting with the colloid, the vesicle is thus able to optimize both its shape and charge distribution. Our objective is to characterize the wrapping transition in terms of the electrostatic screening strength and vesicle bending stiffness. In addition, we briefly investigate the coupling between composition and spontaneous curvature of the vesicle by assigning to the mobile charges on the vesicle a preferential curvature. Our computational investigations are complemented by a minimal phenomenological model. The model correctly predicts the wrapping transition to be discontinuous, although it fails to provide a quantitative description.

II. THEORETICAL MODEL

We consider the electrostatic interaction between a closed fluidlike vesicle and a single spherical colloid. The vesicle is flexible and contains mobile charges; it is thus able to adjust both shape and charge distribution in order to optimize the interaction with the oppositely charged rigid colloid. We model the vesicle as a triangulated surface that contains a fixed number N of vertices of which M vertices are charged. That is, a fraction $\phi=M/N$ of all vertices carry a single negative charge; the remaining vertices are uncharged. The colloid is located outside the vesicle and is represented by a sphere of fixed radius R_{coll} with a given surface charge density σ_{coll}. Both the vesicle and the colloid are embedded in an aqueous solution of uniform dielectric constant ε, bulk concentration n_0 of monovalent salt, and fixed temperature T. It is convenient to express ε and n_0 in terms of the Bjerrum length $l_B=e^2/(4\pi\varepsilon\varepsilon_0 kT)$ and Debye screening length $l_D=(8\pi l_B n_0)^{-1/2}$, respectively, where e denotes the elementary charge, ε_0 is the vacuum permittivity, and k is Boltzmann's constant.

In the present work we model electrostatic interactions conveniently using the linear (Debye–Hückel) screening approximation, which leads to the effective pair potential $u(r)=\pm(l_B/r)\exp(-r/l_D)$ between any two given elementary charges that are separated by distance r. The plus and minus signs correspond to like and unlike charges, respectively. Note that the linear screening approximation neglects charge-charge correlations of the ions in solution, which is strictly valid only in the limit of small electrostatic potential Φ (i.e., when $e\Phi \ll kT$). The use of the linear screening approximation in the present study is still appropriate because we are concerned with the interaction of *oppositely* charged macroions. Charge-charge correlations are not expected to qualitatively alter the nature of the attraction between the vesicle and the oppositely charged colloid.

The energy $\mathcal{H}$ of any given microstate of the colloid-vesicle complex consists of two contributions, the bending energy of the vesicle and the total electrostatic energy. The two terms can be written as

$$\mathcal{H}=\frac{\kappa}{2}\int_A ds(c_1+c_2)^2+\frac{kT}{2}\sum_{i,j} u(|\mathbf{r}_i-\mathbf{r}_j|), \tag{1}$$

where the first part accounts for the bending energy;[17] κ is the bending stiffness and the integration runs over the surface of the closed vesicle with c_1+c_2 being the sum of the local principal curvatures. The second part—the electrostatic contribution—is a sum over all elementary charges located at distinct positions r_i and r_j. Note that the electrostatic self-energy of the rigid colloid is constant (and can thus be omitted). However, the electrostatic self-energy of the vesicle depends on both shape and charge distribution and can therefore not be ignored.

A. Monte Carlo simulations

To study the equilibrium conformations of the colloid-vesicle system we employ a Monte Carlo simulation method. The vesicle is represented by a set of N vertices that are linked by tethers of flexible length l so as to form a closed, randomly triangulated, self-avoiding network.[18] The lengths of the tethers can vary between a minimal (l_{min}) and a maximal (l_{max}) value. This model has been used previously to study shapes and fluctuations of one-component[19,20] and two-component[21–23] vesicles. Membrane fluidity is maintained by flipping bonds within the triangulated network. A single bond flip involves the four vertices of two neighboring triangles. The tether between two vertices is cut and reestablished between the other previously unconnected two vertices. A Monte Carlo step involves attempted changes in vertex positions and bond flips, as described below. Note that the fluidity of the vesicle allows the lateral (in-plane) redistribution of the vertices for any given vesicle shape. In addition, the (out-of-plane) positional freedom of the N vertices enables the vesicle to adjust its shape. Hence, the interaction of the vesicle with the oppositely charged colloid will be optimized with respect to both the vesicle shape and distribution of charged vertices.

The choice for the maximum tether length $l_{\mathrm{max}}=1.68l_{\mathrm{min}}$ ensures self-avoidance of the network. It is

convenient to use $l_{\min}$ as our unit length and to express all lengths in terms of $l_{\min}$. The following system parameters are adopted in our simulations: $R_{\text{coll}}=3$ (radius of the colloid), $l_B=1$ (Bjerrum length), and $h_{\min}=0.5$ (minimal distance between any given vertex and the surface of the colloid). In addition, the spherical colloid carries $N_{\text{coll}}=65$ uniformly distributed, pointlike, positive charges of valence $Z_{\text{coll}}=+2$ on its surface. Our vesicle consists of $N=1447$ vertices [forming $2(N-2)=2890$ triangles], of which a fraction ϕ is negatively charged with valence $Z=1$. The three parameters we have varied in our simulations are the total number M of charged vertices on the vesicle, the Debye screening length l_D, and the bending stiffness κ.

The minimal cross-sectional area per vertex corresponding to $l=l_{\min}=1$ is $a_{\min}\approx\sqrt{3}/2\approx 0.87$. The *average* cross-sectional area per vertex a is significantly larger than the minimal one, $a>a_{\min}$. A rough estimate of a may be based on the assumption that all tether lengths (with $1\le l\le 1.68$) are adopted with the same probability, implying $a\approx 1.5$. This estimate is supported by our Monte Carlo simulations as discussed below. The total vesicle area is $A=aN=2170$, corresponding to a sphere of radius $R=13.1$. The ratio between the area A of the vesicle and the area $A_{\text{coll}}=4\pi R_{\text{coll}}^2$ of the colloid is therefore $A/A_{\text{coll}}=19.2$. We also note that the average cross-sectional area per unit charge on the colloid $a_{\text{coll}}=4\pi R_{\text{coll}}^2/(Z_{\text{coll}}N_{\text{coll}})\approx 0.87$ is equal to $a_{\min}$.

As introduced in Eq. (1), the energy $\mathcal{H}$ of a given microstate of the colloid-vesicle complex is the sum of the bending and electrostatic energies. For the numerical calculation of the bending energy of a triangulated surface, see Sec. II in Ref. 24 or Eq. 70 in Ref. 18. In our Monte Carlo simulations, the microstates of the colloid-vesicle complex are sampled according to the Metropolis algorithm. Evolution of the system is measured in millions of Monte Carlo steps (Mmcs). One Monte Carlo step consists of separate attempts to displace each of the N vertices by a random increment in the cube $[-s,s]^3$, followed by N attempts to flip a randomly chosen bond. We chose $s=0.15$ so that approximately 50% of vertex displacements were successful. We have typically used about 1 Mmcs to measure thermal averages after reaching equilibrium.

B. Phenomenological model

To interpret our computational findings, we construct a minimal phenomenological two-state model for the wrapping of the colloid by the vesicle. We distinguish between two regions of the vesicle. The first region (indexed c—colloid) realizes the partial wrapping of the colloid; its shape is assumed to be the section of a sphere. The second region (indexed b—bulk) does not contribute to the wrapping; its shape is free to adjust. We shall refer to the two regions as wrapping and nonwrapping regions.

The areas of the wrapping and nonwrapping regions are A_c and $A_b=A-A_c$, respectively; we denote the corresponding area fractions by $\theta_c=A_c/A$ and $\theta_b=A_b/A$. The maximal vesicle area that can participate in the wrapping is $A_c^{\max}=4\pi R_c^2$. Here $R_c=R_{\text{coll}}+h$ denotes the radius of curvature of the colloid-wrapping vesicle region (which also accounts for a nonvanishing distance $h\gtrsim h_{\min}$ of closest approach between vesicle and colloid). Clearly, $A_c=A_c^{\max}$ corresponds to the fully wrapped colloid. Intermediate (i.e., partially wrapped) states can be described conveniently by the wrapping parameter

$$\lambda = A_c/A_c^{\max} = \theta_c A/A_c^{\max}, \quad 0\le\lambda\le 1. \tag{2}$$

Each of the two vesicle regions, wrapping and nonwrapping, can be characterized by its number of charged vertices, denoted by M_c and $M_b=M-M_c$, and by the total number of vertices, N_c and $N_b=N-N_c$, respectively. The corresponding compositions (i.e., fractions of charged vertices) are $\phi_c=M_c/N_c$ and $\phi_b=M_b/N_c$. We thus have the charge conservation condition $\theta_c\phi_c/a_c+\theta_b\phi_b/a_b=\phi/a$, where $a_c=A_c/N_c$ and $a_b=A_b/N_b$ denote the average cross-sectional areas per vertex in the wrapping and nonwrapping vesicle regions, respectively.

Our phenomenological model makes a number of simplifying assumptions: (i) fluctuations of the vesicle shape are neglected, only the ground state energy is retained; (ii) compositions in both the wrapping and nonwrapping regions are uniform, and the mixing is ideal; (iii) the vesicle is laterally incompressible, implying $a_c=a_b=a$; (iv) the electrostatic energy of the nonwrapping vesicle region is described by that of a planar charged surface with surface charge density $-e\phi_b/a_b$; (v) the electrostatic energy of the wrapping vesicle region is described by a circular flat surface of radius $\bar{R}_c$ and surface charge density $-e\phi_c/a_c$; (vi) only charges within the wrapping region interact with the colloid, where electrostatic interactions are approximated as with a flat surface at fixed distance $h\gtrsim h_{\min}$ away; and (vii) only bending elasticity, but not electrostatics, determines the vesicle shape of the nonwrapping region. The last of these assumptions can be justified because the electrostatic contribution to the bending stiffness is small.[25] We emphasize, however, that our set of assumptions is introduced phenomenologically, serving the major purpose to keep the model simple.

We decompose the phenomenological free energy of the colloid-vesicle complex $F=F_{\text{mix}}+F_{\text{elec}}+F_{\text{bend}}$ into mixing, electrostatic, and bending contributions. Our assumptions outlined above significantly simplify the calculation of each individual contribution. Specifically, the mixing contribution

$$F_{\text{mix}} = N[\theta_c f_{\text{mix}}(\phi_c) + \theta_b f_{\text{mix}}(\phi_b)] \tag{3}$$

can be expressed in terms of the ideal mixing free energy $f_{\text{mix}}(x)/kT=x\ln x+(1-x)\ln(1-x)$ per vertex.

The electrostatic contribution to the total free energy

$$F_{\text{elec}} = N[\theta_c f_{\text{elec}}^{(c)}(\phi_c) + \theta_b f_{\text{elec}}^{(b)}(\phi_b)] \tag{4}$$

contains the two expressions

$$\frac{f_{\text{elec}}^{(c)}}{kT} = p_0[Z^2\phi_c^2 g(\bar{R}_c) - 2ZZ_{\text{coll}}\phi_c\phi_{\text{coll}}e^{-h/l_D}] \tag{5}$$

and

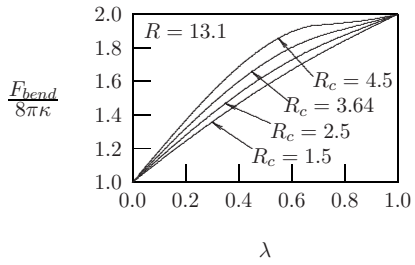

FIG. 1. Bending free energy F_{bend} of a vesicle that partially wraps a spherical colloid of *effective* radius $R_c=R_{\text{coll}}+h$ plotted as a function of the wrapping parameter λ. The surface area of the vesicle $A=4\pi R^2$ corresponds to a sphere of radius R. The method to calculate F_{bend} is outlined in the Appendix. The Monte Carlo simulations of the present work all correspond to the case $R=13.1$ and $R_c=3.64$.

$$\frac{f_{\text{elec}}^{(b)}}{kT} = p_0 Z^2 \phi_b^2, \tag{6}$$

which represent the electrostatic energies per vertex of the wrapping and nonwrapping regions, respectively. The first part on the right-hand side (rhs) of Eq. (5), namely, $p_0 Z^2 \phi_c^2 g(\bar{R}_c)$, describes the electrostatic self-energy per vertex in the wrapping region. Here, $p_0=\pi l_B l_D/a$ is a constant, and the function[26,27]

$$g(\bar{R}_c) = 2\int_0^\infty \frac{dk}{k} \frac{J_1^2(k\bar{R}_c)}{\sqrt{1+(kl_D)^2}} \tag{7}$$

accounts for the finite size of the wrapping region, which we model as a flat surface of circular shape with radius $\bar{R}_c=\sqrt{\lambda A_c^{\max}/\pi}$. $J_1(x)$ is the Bessel function of the first kind, and thus $g(\bar{R}_c)$ is a monotonically increasing function with $g(\bar{R}_c=0)=0$ and $g(\bar{R}_c\to\infty)=1$. The second part on the rhs of Eq. (5), namely, $-2ZZ_{\text{coll}}\phi_c\phi_{\text{coll}}\exp(-h/l_D)$, accounts for the electrostatic interaction free energy of a given vertex in the wrapping region with the colloid, modeled as a flat large surface at a distance $h>h_{\min}=0.5$ away. The magnitude $h=0.64$ has been determined from our simulations, see below. Finally, $f_{\text{elec}}^{(b)}$ in Eq. (6) represents the electrostatic self-energy per vertex in the nonwrapping region. No additional factor g, analogous to Eq. (7), is needed since we only consider vesicles considerably larger than the Debye length.

The final contribution $F_{\text{bend}}=(\kappa/2)\int_A ds(c_1+c_2)^2$ is the elastic energy of bending. κ is the nonelectrostatic contribution to the bending stiffness; the electrostatic contribution is neglected as pointed out above. The vesicle forms a spherical cap in the colloid-wrapping region; the corresponding elastic energy is $8\pi\kappa\lambda$. In the nonwrapping region, the contribution to the bending energy is $8\pi\kappa$ for both $\lambda=0$ and $\lambda=1$. Hence $F_{\text{bend}}/(8\pi\kappa)=1$ for $\lambda=0$ and $F_{\text{bend}}/(8\pi\kappa)=2$ for $\lambda=1$. Calculation of the energy F_{bend} for intermediate λ is based on optimizing the shape of an axisymmetric vesicle of fixed area A in the ground state. The corresponding shape equations are stated in the Appendix. Note that our minimization neither constrains the volume enclosed in the vesicle (see Ref. 28 for numerical shape optimization at fixed volume) nor accounts for the so-called area difference elasticity.[29] The behavior of $F_{\text{bend}}(\lambda)$ depends only on the ratio R/R_c. Figure 1 displays a number of numerical results for $F_{\text{bend}}(\lambda)$. Included is a curve for the specific choices $R=13.1$ and $R_c=3.64$, which corresponds to our Monte Carlo simulations and is thus used in our phenomenological model. Vesicle shapes corresponding to $\lambda=0.15$, $\lambda=0.5$, and $\lambda=0.975$ are shown in Fig. 2 below. Note that in the limit $R\gg R_c$ the bending energy is $F_{\text{bend}}=8\pi\kappa(1+\lambda)$. In this case, the excess deformation of the vesicle in the nonwrapping region is catenoidlike and thus does not imply an additional energy penalty.

Our phenomenological model describes the free energy of the colloid-vesicle complex in terms of ϕ_b, ϕ_c, θ_b, and θ_c [or, instead of θ_c, equivalently by λ; see Eq. (2)]. With the two conservation conditions $\theta_c\phi_c+\theta_b\phi_b=\phi$ and $\theta_c+\theta_b=1$, this leaves two degrees of freedom which we chose to be λ and ϕ_c. The phenomenological free energy $F=F(\lambda,\phi_c)$ adopts the global minimum with respect to these two degrees of freedom. We have determined this minimum numerically.

III. RESULTS AND DISCUSSION

Recall that apart from the number of charged vertices M (or, equivalently, fraction of charged vertices ϕ), Debye screening length l_D, and bending stiffness κ, all parameters of the system have been specified. We describe the degree of wrapping as a function of M for different l_D and κ.

Figure 2 illustrates a number of typical conformations of the colloid-vesicle complex as obtained by the Monte Carlo

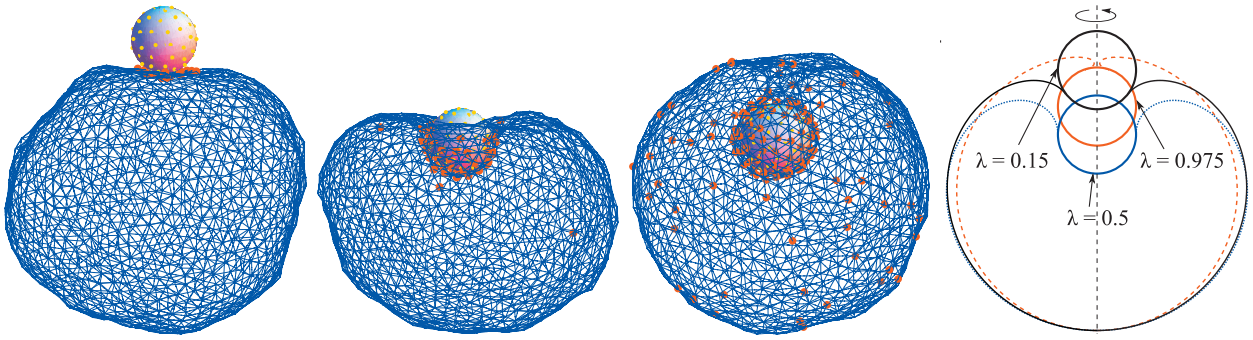

FIG. 2. The wrapping of a colloid (radius $R_{\text{coll}}=3$) by a vesicle (which, if spherical, would have a radius of $R=13.1$). Left: snapshots of representative colloid-vesicle configurations obtained from simulations for different numbers of charged vertices on the membrane: $M=15$, $M=60$, and $M=150$ (from left to right). The shape of the vesicle is represented by a triangulated surface; mobile charges on the vesicle and fixed charges on the colloid are indicated by dots. Right: cross sections of colloid-vesicle complexes obtained by minimizing the bending energy of the vesicle (see Appendix) for different values of the wrapping parameter λ.

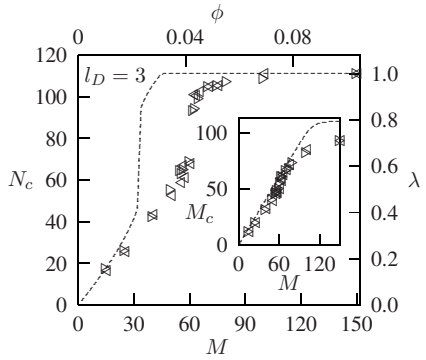

FIG. 3. Number of vertices in the wrapping region N_c as a function of the total number M of charged vertices in the vesicle. Results from Monte Carlo simulations are marked by the symbols ▹ and ◃, corresponding to fully unwrapped and fully wrapped initial states of the simulation run, respectively. At about $\phi=0.04$ a discontinuous wrapping transition occurs. The dashed line is the prediction of our phenomenological model. The inset shows the number of charged vertices in the wrapping region M_c. All results correspond to $l_D=3$ and $\kappa=10kT$.

simulations. The three complexes correspond to $M=15$, $M=60$, and $M=150$ (from left to right), all simulated for $l_D=3$ and $\kappa=10kT$. For all three simulations we have measured the wrapping parameter λ. [Note that in our simulations a vertex is taken to reside within the wrapping region if its distance from the colloid is less than 1.5, measured in our unit length $l_{\min}$. We then calculated the corresponding vesicle shapes using our phenomenological model (thus minimizing F_{bend})]. Cross sections of the resulting vesicle shapes are displayed in the right diagram of Fig. 2.

The snapshots of the Monte Carlo simulations in Fig. 2 indicate an interplay between the degree of wrapping and charge segregation on the vesicle surface. All charges are sequestered close to the colloid for $M=15$; the colloid is adsorbed to the vesicle, but the degree of wrapping is small ($\lambda=0.15$). The choice $M=60$ corresponds to almost half the number $Z_{\text{coll}}N_{\text{coll}}=2\times65=130$ of elementary charges on the colloid. With nearly complete segregation of charged and uncharged vertices, this suggests a wrapping parameter $\lambda=1/2$ for $M=60$. Note that very few charges appear to have escaped the membrane-wrapping region due to thermal fluctuations; these charges move essentially unrestricted within the nonwrapping part of the vesicle surface. Finally, for $M=150$ the vesicle charge overcompensates that on the colloid, leading to complete wrapping and a residual fraction of charged vertices on the nonwrapping part of the vesicle surface.

To study whether the transition from small to large degrees of wrapping is discontinuous, we performed simulations for various M, all at fixed Debye length $l_D=3$ and bending stiffness $\kappa=10kT$. Figure 3 displays the number N_c of vertices in the wrapping region and—in the inset—the corresponding number of charged vertices M_c in the wrapping region, both plotted as a function of the total number of charged vertices M or, equivalently, as a function of the composition $\phi=M/N$. The right axis in Fig. 3 indicates the wrapping parameter $\lambda=N_c a/A_c^{\max}$ with $A_c^{\max}=4\pi(R_{\text{coll}}+h)$. Here the distance $h=0.64$ is chosen so as to match the maximal wrapping parameter $\lambda=1$ to the case of complete wrapping in the simulations. We have also reproduced the value $h=0.64$ by measuring the colloid-to-vesicle distance in the wrapped region for different simulations. Note that due to thermal fluctuations $h=0.64$ is somewhat larger than $h_{\min}=0.5$.

The two different sets of symbols in Fig. 3 correspond to two sets of Monte Carlo simulation runs with different initial states, one fully unwrapped (▹) and the other fully wrapped (◃). No hysteresis is observed which indicates the absence of two distinct minimum states (weakly and fully wrapped) that are separated by a barrier much larger than the thermal energy. At about $\phi=0.04$ there is a discontinuous wrapping transition in qualitative agreement with the predictions of corresponding elasticity models.[10] Electrostatic interactions are strong enough to draw almost every charged vertex into the wrapping region, as shown in the inset of Fig. 3. Hence, the number of charged vertices in the wrapping region changes continuously; $M_c\approx M$. What changes discontinuously during the wrapping transition is the number of *uncharged* vertices. Thus, the wrapping transition mainly involves a dilution of charges in the wrapping region.

The dashed line in Fig. 3 marks the prediction of our phenomenological model. As in the simulations, a discontinuous wrapping transition is predicted, although at significantly smaller M. We bring forward two major reasons for this difference. First, the discretized structure of the vesicle in the simulations leads to a wider neck at larger wrapping parameters than predicted by the phenomenological model. The corresponding additional energy cost of the (discretized) vesicle neck disfavors large wrapping and thus delays the wrapping transition in the simulations. Second, in the Monte Carlo simulations, some charged vertices reside close to the colloid without entering the wrapping region. The favorable electrostatic interaction of these charged vertices with the colloid (which does not require an increase in λ) is ignored in the phenomenological (two-state) model. Hence, wrapping in the simulations tends to be less pronounced than in the two-state model. We note that the presence of a discontinuous wrapping transition in our phenomenological model depends crucially on the nonlinear behavior of the bending energy $F_{\text{bend}}(\lambda)$ in Fig. 1. Using the linear function $F_{\text{bend}}=8\pi\kappa(1+\lambda)$, which is valid in the limit of a small colloid ($R_c\ll R$), would eliminate the discontinuity of the wrapping. It is less important to account for the finite size of the wrapping region in calculating the electrostatic self-energy. Setting $g(\bar{R}_c)\equiv1$ in Eq. (5) would preserve the discontinuity of the wrapping, but the transition would be shifted to even smaller ϕ.

Our next set of simulations was carried out for a Debye length of $l_D=1$. Decreasing l_D corresponds to an increase in electrostatic screening and thus to weaker electrostatic interactions. Consequently, a larger number M of charged vertices is required to wrap the colloid. Results from our simulations and phenomenological model are displayed in Fig. 4. Again, as in Fig. 3, the two sets of symbols correspond to results of simulation runs with fully unwrapped (▹) and fully wrapped (◃) initial states of the colloid-vesicle complex. In contrast to Fig. 3, the simulation results in Fig. 4 exhibit hysteresis. Simulation runs starting from the fully unwrapped initial

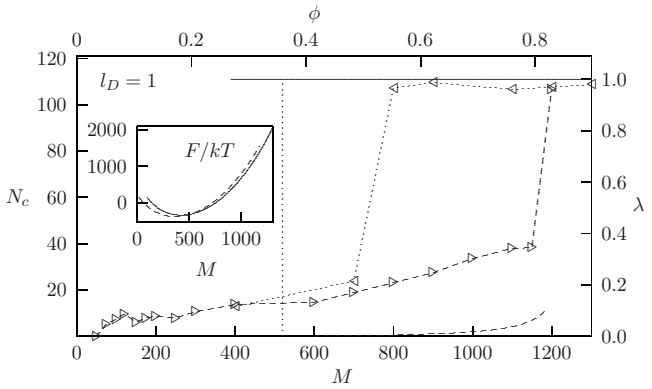

FIG. 4. Number of vertices in the wrapping region N_c as a function of the total number M of charged vertices in the vesicle. Results from Monte Carlo simulations are marked by the symbols ▹ (connected by dashed lines) and ◃ (connected by dotted lines), corresponding to fully unwrapped and fully wrapped initial states of the simulation run, respectively. The two minimum states predicted by the phenomenological model are marked by the solid line and the dashed curve for the full and weak wrapping regimes, respectively. The inset shows the corresponding free energy F. At $M=500$ (see the vertical dotted line in the main figure) both states have the same free energy. All results correspond to $l_D=1$ and $\kappa=10kT$.

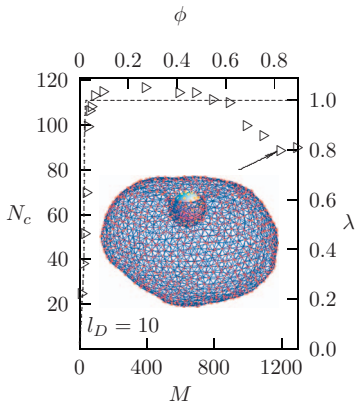

FIG. 5. Number of vertices in the wrapping region N_c as a function of the total number M of charged vertices in the vesicle. Results from Monte Carlo simulations (▹) are shown together with the prediction (dashed line) from the phenomenological model. The inset displays a representative colloid-vesicle complex corresponding to $M=1200$. All results correspond to $l_D=10$ and $\kappa=10kT$.

state (symbol ▹ in Fig. 4) lead to a wrapping transition at $M\approx1200$. On the other hand, when starting from the fully wrapped state (symbol ◃ in Fig. 4), the unwrapping transition takes place at $M\approx800$. Apparently, two local minimum states exist that are separated by a large energy barrier. For $l_D=1$ the wrapping transition is more pronounced than for $l_D=3$; i.e., the initial and final states of the transition correspond to almost vanishing and complete wrapping, respectively.

Some, but not all, of our computational findings for $l_D=1$ (see Fig. 4) are reproduced by the phenomenological model. The model does predict two minima of the free energy, one for small degree of wrapping (indicated by the dashed line in Fig. 4) and the other for full wrapping (see the horizontal solid line in Fig. 4 at $\lambda=1$). The free energies corresponding to the two local minima are displayed in the inset of Fig. 4. At about $M=M_{\mathrm{crit}}=500$ both minima have the same free energy (marked by the vertical dotted line in Fig. 4). For $M<M_{\mathrm{crit}}$ the almost completely unwrapped state is thermodynamically stable; $M>M_{\mathrm{crit}}$ implies stability of the fully wrapped colloid. Although the phenomenological model correctly predicts the presence of a pronounced discontinuous wrapping transition, it cannot reproduce its quantitative features. It is also worth pointing out that in the weakly wrapped regime the simulations predict a notable (and nearly linearly increasing) degree of wrapping as function of M, reaching almost $\lambda=0.4$ for $M=1200$. In comparison, the degree of wrapping predicted by the phenomenological model is almost negligible. This is especially interesting because for $l_D=3$ (discussed above; see Fig. 3) the phenomenological model overestimates λ in the weakly wrapped regime. The underestimation of λ for $l_D=1$ may result from our model's assumption that the wrapping region adopts the shape of a spherical cap of fixed radius $R_{\mathrm{coll}}+h$. In the simulations, the membrane shape fluctuates, allowing vesicle configurations with lower bending energy, but with charged vertices still close to the vesicle.

We have also carried out a set of simulations for large Debye lengths, namely, $l_D=10$. The results are displayed in Fig. 5. Also shown (dashed line) is the prediction of our phenomenological model. Two features are notable. First, the large Debye length only moderately affects the wrapping transition as compared to $l_D=3$ (see Fig. 3). That is, we observe a discontinuous wrapping transition at about $M=55$ with N_c jumping from 70 to 100; the phenomenological model also predicts this transition at $M=30$ from $N_c=45$ to $N_c=95$. Second, increasing M beyond the wrapping transition leads to an initial increase in N_c followed by a substantial decrease. The wrapping parameter corresponding to the maximal value of N_c is found to be larger than $\lambda=1$. This is a consequence of our assumption that the cross-sectional area per vertex $a_c=a$ in the definition of the wrapping parameter $\lambda=N_c a_c/4\pi R_c$ is a constant. However, in our simulations we observe a decrease in a_c. Specifically, at $M=400$ the cross-sectional area per vertex a_c is about 10% smaller than that in the bulk region of the vesicle. Hence, additional vertices can be accommodated into the wrapping region, which allows for $\lambda>1$. For even larger M, the degree of wrapping decreases; a representative colloid-vesicle complex corresponding to $M=1200$ is shown in the inset of Fig. 5. The gradual unwrapping for large l_D and M is the result of electrostatic repulsion within the vesicle neck. Indeed, for a similar system—the ground state of a homogeneously charged colloid-membrane complex at large l_D—unwrapping has been predicted by Fleck and Netz.[7]

Consider now changing the bending stiffness κ of the vesicle at fixed Debye length $l_D=3$. In Fig. 3 we have already observed that a discontinuous wrapping transition takes place for $\kappa=10kT$ at about $M=M_{\mathrm{crit}}=60$. In Fig. 6 we show that the number M_{crit} increases linearly with the bending stiffness. That is, more charged vertices are needed to induce the wrapping transition of a stiffer membrane. However, for decreasing bending stiffness (at about $\kappa=3kT$) the wrapping transition terminates in a critical point. The presence of a critical point can also be seen in the inset of Fig. 6, which shows the free energy as a function of N_c at the wrap-

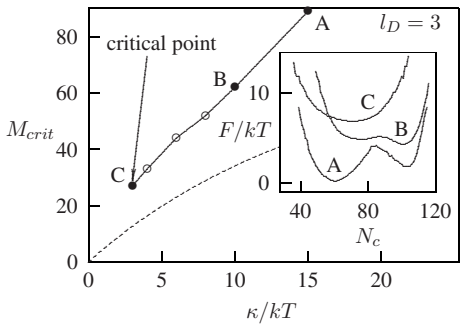

FIG. 6. The number of charged vertices M_{crit} required to induce a discontinuous wrapping transition as a function of the bending stiffness κ. Data points from our simulations are connected by straight lines. The inset shows the free energy $F=F_0-kT\ln p(N_c)$ corresponding to points A (for $\kappa=15kT$), B (for $\kappa=10kT$), and C (for $\kappa=3kT$); F_0 is a reference energy and $p(N_c)$ is the probability to find N_c vertices within the wrapping region. We have measured that probability from our simulations. Note that our computational results for $M_{\mathrm{crit}}(\kappa)$ indicate a critical point at about $\kappa=3kT$. No critical point is predicted by our phenomenological model (dashed line). All results are derived from the Debye length $l_D=3$.

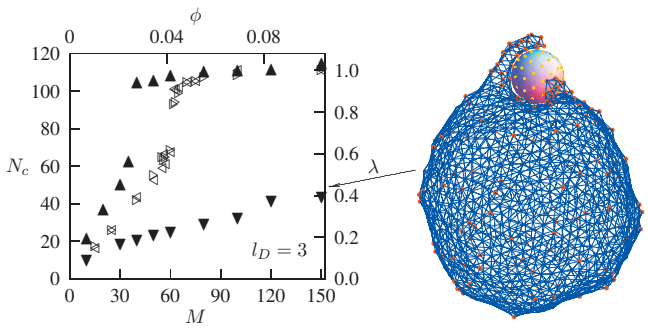

FIG. 7. Simulation results for the number of vertices in the wrapping region N_c as a function of the total number M of charged vertices in the vesicle. The two data sets ▲ and ▼ correspond to the two spontaneous curvatures $c_0=-2/R_{\mathrm{coll}}$ and $c_0=+2/R_{\mathrm{coll}}$ of a fully charged vesicle segment. Results for the absence of composition-curvature coupling ($c_0=0$) marked by ▷ and ◁ are replotted from Fig. 3. A representative colloid-vesicle complex for $M=150$ and $c_0=+2/R_{\mathrm{coll}}$ is also shown. All results correspond to $l_D=3$ and $\kappa=10kT$.

ping transition (corresponding to $M=M_{\mathrm{crit}}$) derived from the simulations. Specifically, for three different bending stiffnesses (marked by A, B, and C) we have identified $M=M_{\mathrm{crit}}$ and then measured the probability $p(N_c)$ to find a certain degree of wrapping as expressed by the number N_c of vertices in the wrapped region. The corresponding change in free energy $F-F_0=-kT\ln p$ displayed in the inset of Fig. 6 exhibits two minima for large bending stiffness (A and B), which have merged into a single minimum for $\kappa=3kT$ (curve C). The height of the barrier that separates the two minima grows with increasing κ but is still comparable to the thermal energy kT at $\kappa=10kT$. This is consistent with the absence of hysteresis in Fig. 3. We have also calculated $M_{\mathrm{crit}}(\kappa)$ from our phenomenological model, see the dashed line in Fig. 6. Note that the phenomenological model does not predict a critical point. This is because membrane undulations are not taken into account in the phenomenological model and even a small energy barrier is enough to separate partially and the fully wrapped energy states.

We finally consider the influence of an additional nonelectrostatic composition-curvature coupling of the vesicle. To this end, we assume that the charged vertices (but not the uncharged vertices) possess a nonvanishing preferential intrinsic curvature c_0.[30,31] The presence of a composition-dependent spontaneous curvature of the vesicle can be described by adding the term

$$-c_0\kappa\int_A ds\,\eta(c_1+c_2) \tag{8}$$

to the energy expression $\mathcal{H}$ of any given microstate in Eq. (1). It is $\eta=1$ if the lateral area corresponding to a given vertex is charged and $\eta=0$ if it is uncharged. Hence, only charged vertices contribute to the integration over the surface of the triangulated vesicle. We note that Eq. (8) is based on the assumption that the spontaneous curvature of the mixed membrane ηc_0 depends linearly on composition; such an assumption finds support by comparison of model calculations with experimental studies[32] and with molecular lipid models.[33] Depending on the sign of c_0 wrapping of the colloid by charged vertices will either be favored (for $c_0<0$) or disfavored (for $c_0>0$). We have carried out simulations for both cases, assuming the magnitude of the spontaneous curvature to be $|c_0|=2/R_{\mathrm{coll}}$. Simulation results are shown in Fig. 7. For preferential matching of charged vertices with the colloid $c_0=-2/R_{\mathrm{coll}}$ (corresponding to the symbol ▲ in Fig. 7), we observe enhanced degree of wrapping as compared to the case $c_0=0$. That is, a more pronounced discontinuous wrapping transition occurs at smaller M; compare $M_{\mathrm{crit}}=40$ for $c_0=-2/R_{\mathrm{coll}}$ to $M_{\mathrm{crit}}=60$ for $c_0=0$. In the opposite case, for $c_0=+2/R_{\mathrm{coll}}$ (corresponding to the symbol ▼ in Fig. 7), charged vertices in the wrapping region are penalized. This completely eliminates the wrapping transition. Instead, for large M, we observe a nonaxisymmetric clamplike configuration such as that displayed in Fig. 7.

IV. CONCLUSIONS

In this work we have presented Monte Carlo simulations of a fluid vesicle that internalizes a spherical colloid by a wrapping process. The wrapping is driven by screened electrostatic interactions between the colloid and the oppositely charged vesicle. Only a fraction ϕ of the vesicle's mobile vertices are charged. Hence, the engulfment of the colloid is coupled to the lateral segregation of vesicle charges. The present Monte Carlo simulations complement the preceding investigations of colloid wrapping by fluid membranes based on various other methods, as discussed in Sec. I.

Here, we summarize our major findings. As predicted for colloids that interact with a membrane by a short-ranged adhesive potential,[8–10] our system typically exhibits a *discontinuous* wrapping transition from a partial to complete (or almost complete) degree of wrapping. The two energetically preferred states, partially and completely wrapped, can be separated by an energy barrier significantly larger than the thermal energy kT, implying the observation of hysteresis in our simulations. If the electrostatic screening length l_D is increased, the transition shifts to smaller ϕ and becomes weaker, i.e., with a smaller energy barrier and no hysteresis. We also observe a reentrant wrapping-unwrapping behavior

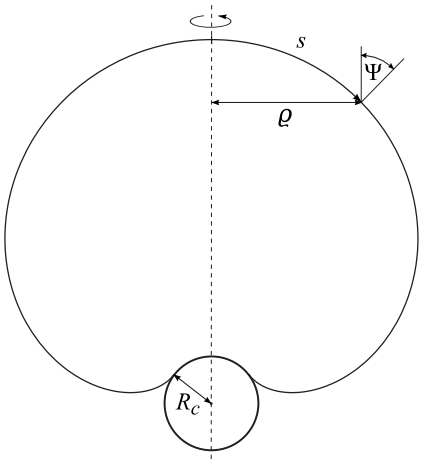

FIG. 8. Shape of a rotationally symmetric vesicle that partially wraps a spherical colloid of radius R_c. The arc length s and the functions $\varrho(s)$ (distance from the axis of symmetry) and $\Psi(s)$ (angle between the vesicle normal and the axis of symmetry) are indicated. The optimal shape is calculated as outlined in the Appendix.

for large l_D upon increasing ϕ. This behavior has been predicted previously by Fleck and Netz[7] for a uniformly charged membrane. Decreasing the bending stiffness of the vesicle weakens the wrapping transition until a critical point is reached beyond which the wrapping becomes a continuous process. Finally, the wrapping transition shifts to smaller ϕ if the charged vertices possess a spontaneous curvature that matches the curvature of the colloid. In the opposite case, when the spontaneous curvature of the charged vertices is opposite to the curvature of the colloid, the wrapping is a continuous process. Interestingly, the preferred shape of the vesicle then becomes clamplike and nonaxisymmetric.

To facilitate the discussion of our computational findings, we have suggested a minimal phenomenological model. The corresponding free energy of the colloid-vesicle complex contains a demixing, electrostatic, and bending contribution, all calculated using a significant number of simplifying assumptions. Still, our model is able to recapture the discontinuity of the wrapping transition, although without achieving quantitative agreement with our simulation results.

The engulfment of a colloidal particle by a fluid membrane is a fundamental process with relevance to cellular drug uptake, viral budding, and biotechnological applications. As in previous modeling studies, the present simulations adopt drastic simplifications in order to extract generic features of the wrapping process. These include the use of a screened electrostatic (i.e., Yukawa) potential, which ignores correlations and overestimates electrostatic interactions as compared to nonlinear Poisson–Boltzmann theory. Moreover, spatial variations in the dielectric constant are not accounted for in the present model. Finally, the triangulated surface model neglects the molecular structure of the vesicle's constituents and ignores the possibility of topological changes. On the other hand, our simulations go beyond previous phenomenological models by accounting for thermal fluctuations and for the lateral mobility of the charged vertices. It is thus notable that previous predictions, such as the discontinuous nature of the wrapping transition or the reentrant wrapping-unwrapping process for large screening lengths, agree with the findings of the present work.

ACKNOWLEDGMENTS

S.M. thanks the NSF for support through Grant No. DMR-0605883; D.M.K. acknowledges the support from the NSF under Grant Nos. DMR-0513393 and DMR-0706017. The authors also acknowledge the support of the Slovenian Research Agency through Grant No. BI-U.S./08-10/072.

APPENDIX: SHAPE EQUATIONS

We consider an axisymmetric vesicle that adopts the shape of a spherical cap in the colloid-wrapping region. Figure 8 displays a cross section of the colloid-vesicle complex. It is convenient to describe the vesicle shape as a function of the contour length s of the vesicle's cross section using the distance $\varrho=\varrho(s)$ to the axis of symmetry and the angle $\Psi=\Psi(s)$ between the normal of the vesicle surface and the axis of symmetry. The two principal curvatures of the vesicle are the $c_1=d\Psi/ds$ and $c_2=\sin\Psi/\varrho$. The bending energy of the vesicle can thus be written as

$$F_{\text{bend}} = 8\pi\kappa\lambda + 2\pi\frac{\kappa}{2}\int\left(\frac{d\Psi}{ds}+\frac{\sin\Psi}{\varrho}\right)^2\varrho ds, \tag{A1}$$

where the two contributions account for the wrapped and unwrapped regions of the vesicle; κ is the bending stiffness and λ is the degree of wrapping. We seek to minimize the functional

$$S=\frac{F_{\text{bend}}}{8\pi\kappa}+\frac{\lambda_a}{2}\int\varrho ds+\int\lambda_s(s)\left(\frac{d\varrho}{ds}-\cos\Psi\right)ds, \tag{A2}$$

where λ_a and $\lambda_s(s)$ are Lagrangian multipliers. The first one λ_a ensures conservation of the area $A_b=2\pi\int\varrho ds$ of the unwrapped (bare) vesicle region. The second multiplier $\lambda_s(s)$ enforces the geometric relation $\cos\Psi=d\varrho/ds$. The Euler–Lagrange (shape) equations corresponding to S can be written as

$$\begin{aligned}
\varrho' &= \cos\Psi,\\
\Psi' &= \chi/\varrho,\\
\chi' &= \sin\Psi\cos\Psi/\varrho+4\lambda_s\sin\Psi,\\
\lambda_s' &= (\chi^2-\sin^2\Psi)/(8\varrho^2)+\lambda_a/2,
\end{aligned} \tag{A3}$$

where the prime denotes the first derivative with respect to s and where we have defined the function $\chi=\varrho\Psi'$. Equation (A3) can be solved numerically within a range $s_{\min}\le s\le s_{\max}$ subject to appropriate initial conditions. Here, $s_{\min}=\delta\to 0$ corresponds to the top of the vesicle, as shown in Fig. 8, and $s_{\max}$ denotes the contour point where the vesicle establishes a close contact with the spherical colloid. At $s=s_{\min}$ we specify the initial conditions $\varrho(s_{\min})=\delta$, $\Psi(s_{\min})=b\delta$, $\chi(s_{\min})=b\delta$, and $\lambda_s(s_{\min})=0$. The constants b and λ_a can be determined from the two matching conditions at $s=s_{\max}$,

$$\varrho(s_{\max}) = 2R_c\sqrt{\lambda(1-\lambda)},$$

$$\Psi(s_{\max}) = \pi + \sin^{-1}(2\sqrt{\lambda(1-\lambda)}) \quad (\lambda < 0.5), \tag{A4}$$

$$\Psi(s_{\max}) = 2\pi - \sin^{-1}(2\sqrt{\lambda(1-\lambda)}) \quad (\lambda > 0.5).$$

Inserting the solutions for $\Psi(s)$ and $\varrho(s)$ into Eq. (A1) allows us to calculate F_{bend}.

[1] A. Cooper, N. Paran, and Y. Shaul, Biochim. Biophys. Acta **1614**, 89 (2003).
[2] D. D. Lasič and D. Papahadjopoulos, Science **267**, 1275 (1995).
[3] H. Hägerstrand, M. Danieluk, M. Bobrowska-Hägerstrand, V. Pector, J. M. Ruysschaert, V. Kralj-Iglič, and A. Iglič, Biochim. Biophys. Acta **1421**, 125 (1999).
[4] A. J. Lin, N. L. Slack, A. Ahmad, C. X. George, C. E. Samuel, and C. R. Safinya, Biophys. J. **84**, 3307 (2003).
[5] A. L. Troutier and C. Ladaviere, Adv. Colloid Interface Sci. **133**, 1 (2007).
[6] D. Harries, A. Ben-Shaul, and I. Szleifer, J. Phys. Chem. B **108**, 1491 (2004).
[7] C. C. Fleck and R. R. Netz, Europhys. Lett. **67**, 314 (2004).
[8] M. Deserno and T. Bickel, Europhys. Lett. **62**, 767 (2003).
[9] M. Deserno, J. Phys.: Condens. Matter **16**, S2061 (2004).
[10] M. Deserno, Phys. Rev. E **69**, 031903 (2004).
[11] S. A. Nowak and T. Chou, Phys. Rev. E **78**, 021908 (2008).
[12] H. J. Gao, W. D. Shi, and L. B. Freund, Proc. Natl. Acad. Sci. U.S.A. **102**, 9469 (2005).
[13] R. Zhang and T. T. Nguyen, Phys. Rev. E **78**, 051903 (2008).
[14] T. Chou, Biophys. J. **93**, 1116 (2007).
[15] K. A. Smith, D. Jasnow, and A. C. Balazs, J. Chem. Phys. **127**, 084703 (2007).
[16] B. J. Reynwar, G. Illya, V. A. Harmandaris, M. M. Muller, K. Kremer, and M. Deserno, Nature (London) **447**, 461 (2007).
[17] W. Helfrich, Z. Naturforsch. C **28**, 693 (1973).
[18] G. Gompper and D. M. Kroll, in *Statistical Mechanics of Membranes and Surfaces*, 2nd ed., edited by D. Nelson, T. Piran, and S. Weinberg (World Scientific, Singapore, 2004), pp. 359–426.
[19] D. M. Kroll and G. Gompper, Science **255**, 968 (1992).
[20] G. Gompper and D. M. Kroll, J. Phys.: Condens. Matter **9**, 8795 (1997).
[21] P. B. S. Kumar and M. Rao, Phys. Rev. Lett. **80**, 2489 (1998).
[22] P. B. S. Kumar, G. Gompper, and R. Lipowsky, Phys. Rev. Lett. **86**, 3911 (2001).
[23] T. Kohyama, D. M. Kroll, and G. Gompper, Phys. Rev. E **68**, 061905 (2003).
[24] G. Gompper and D. M. Kroll, J. Phys. I **6**, 1305 (1996).
[25] H. N. W. Lekkerkerker, Physica A **159**, 319 (1989).
[26] M. D. Betterton and M. P. Brenner, Phys. Rev. Lett. **82**, 1598 (1999).
[27] A. Iglič and V. Kralj-Iglič, in *Advances in Planar Lipid Bilayers and Liposomes*, edited by A. L. Liu (Elsevier, New York, 2007), Vol. 6, pp. 1–28.
[28] W. T. Gozdz, Langmuir **23**, 5665 (2007).
[29] U. Seifert, Adv. Phys. **46**, 13 (1997).
[30] V. Kralj-Iglič, S. Svetina, and B. Žekš, Eur. Biophys. J. **24**, 311 (1996).
[31] V. Kralj-Iglič, V. Heinrich, S. Svetina, and B. Žekš, Eur. Phys. J. B **10**, 5 (1999).
[32] D. Andelman, M. M. Kozlov, and W. Helfrich, Europhys. Lett. **25**, 231 (1994).
[33] S. May and A. Ben-Shaul, J. Chem. Phys. **103**, 3839 (1995).